2016

Prenatal carbon monoxide impairs migration of interneurons into the cerebral cortex

John F. Trentini
Uniformed Services University

J. Timothy O'Neill
Uniformed Services University

Sylvie Poluch
Uniformed Services University

Sharon L. Juliano
Uniformed Services University

NeuroToxicology 53 (2016) 31–44

Contents lists available at ScienceDirect

NeuroToxicology

Full length article

Prenatal carbon monoxide impairs migration of interneurons into the cerebral cortex

John F. Trentini [a], J. Timothy O'Neill [a,b], Sylvie Poluch [a,c], Sharon L. Juliano [a,c,*]

[a] Graduate Program in Neuroscience, Uniformed Services University, Bethesda, MD 20814, USA
[b] Department of Pediatrics, Uniformed Services University, Bethesda, MD 20814, USA
[c] Department of Anatomy, Physiology and Genetics, Uniformed Services University, Bethesda, MD 20814, USA

ARTICLE INFO

Article history:
Received 12 January 2015
Received in revised form 9 November 2015
Accepted 9 November 2015
Available online 12 November 2015

Keywords:
Carbon monoxide
Neocortical development
Neuronal migration
BrdU
Interneuron

ABSTRACT

Prenatal exposure to carbon monoxide (CO) disrupts brain development, however little is known about effects on neocortical maturation. We exposed pregnant mice to CO from embryonic day 7 (E7) until birth. To study the effect of CO on neuronal migration into the neocortex we injected BrdU during corticogenesis and observed misplaced BrdU+ cells. The majority of cells not in their proper layer colocalized with GAD65/67, suggesting impairment of interneuron migration; interneuron subtypes were also affected. We subsequently followed interneuron migration from E15 organotypic cultures of mouse neocortex exposed to CO; the leading process length of migrating neurons diminished. To examine an underlying mechanism, we assessed the effects of CO on the cellular cascade mediating the cytoskeletal protein vasodilator-stimulated phosphoprotein (VASP). CO exposure resulted in decreased cGMP and in a downstream target, phosphorylated VASP. Organotypic cultures grown in the presence of the phosphodiesterase inhibitor IBMX resulted in a recovery of the leading processes. These data support the idea that CO acts as a signaling molecule and impairs function and neuronal migration by acting through the CO/NO–cGMP pathway. In addition, treated mice demonstrated functional impairment in behavioral tests.

Published by Elsevier Inc.

1. Introduction

The prevalence of maternal smoking remains surprisingly high, ranging from 10 to 50% of pregnant women across different countries and socioeconomic groups (Toro et al., 2008). Prenatal exposure to cigarette smoke associates with a number of adverse clinical effects such as decreased weight and head circumference at birth (Kallen, 2000; Ward et al., 2007), as well as adverse neurological outcomes including increased risk for Sudden Infant Death Syndrome (Pinho et al., 2008) and attention deficit disorder (Milberger et al., 1998). The negative effects of maternal smoking are generally attributed to two major components of cigarette smoke: nicotine and carbon monoxide (CO). While substantial research demonstrates the biological consequences of maternal smoking, the vast majority of studies focus on the effects of nicotine, and often overlook the effects of CO.

Exposure to CO *in utero* causes profound effects in multiple regions of the developing brain, including the basal ganglia, cerebellum, hippocampus, cerebral cortex, and developing white matter (Ginsberg and Myers, 1976; Daughtrey and Norton, 1982; Mereu et al., 2000; Weiss et al., 2004; Benagiano et al., 2005). These effects are attributed to the ability of CO to produce hypoxia at low concentrations. CO also acts as a gaseous signaling molecule similar to nitric oxide (NO). At elevated intracellular levels, CO binds to all heme containing molecules including mitochondrial cytochromes, cytochrome P450, neuroglobin, and cytoglobin (Caughey, 1970; Sawai et al., 2005; Fago et al., 2006). The signaling role for CO first emerged from observations in smooth muscle cells indicating that CO stimulates soluble guanylate cyclase (sGC) to produce cGMP (Furchgott and Jothianandan, 1991). cGMP is an important second messenger for a number of developmental processes including neural plate responsiveness to Sonic hedgehog signaling (Robertson et al., 2001), neuronal growth cone extension, and responsiveness to semaphorin 3A (Song et al., 1998; Van Wagenen and Rehder, 2001). cGMP also activates cGMP dependent kinases, which phosphorylate important cytoskeletal proteins involved in neuronal migration, such as the actin associated cytoskeletal complex Ena/Vasodilator-stimulated phosphoprotein

* Corresponding author at: Corresponding author at: USUHS, 4301 Jones Bridge Road, Bethesda, MD 20810, USA. Tel.: +1 301 295 3673.
E-mail address: sharon.juliano@usuhs.edu (S.L. Juliano).

http://dx.doi.org/10.1016/j.neuro.2015.11.002
0161-813X/Published by Elsevier Inc.

(VASP) (Goh et al., 2002). These processes are essential for brain development. Few have examined the direct effects of CO as a signaling molecule and its role in neuronal migration, a critical component of neocortical development (Knipp and Bicker, 2009). Therefore, this study examined the effects of prenatal CO exposure on the developing neocortex and characterized the structural and functional consequences.

Neocortical development involves the proliferation of neural stem cells followed by migration, and differentiation of neurons in a precisely regulated process. In mice, and mammals in general, the timing of this process is well characterized. Exposure to environmental toxins such as cigarette smoke (Gospe et al., 1996), cocaine (Crandall et al., 2004; Lee et al., 2011; McCarthy et al., 2011), alcohol (Kumada et al., 2007), bisphenol (Nakamura et al., 2007), methyl mercury (Choi et al., 1978), radiation (Algan and Rakic, 1997), methylazoxy methanol (Poluch et al., 2008) or ultrasound (Ang et al., 2006) can result in a myriad of cortical defects based on abnormal proliferation and migration, aberrant cell death patterns, or abnormal gliogenesis (Kriegstein, 1996; Krauss et al., 2003; Pang et al., 2008; McCarthy et al., 2011).

Although the results of prenatal CO exposure have been studied in the brain, the specific effects on neocortical development and neuronal migration have not. Here we report that prenatal exposure to levels of CO similar to that seen in heavy smokers results in displaced cells born during early and late neurogenesis (E12 or E16) in the mouse. Furthermore, CO exposure causes alterations in the distribution of GABAergic interneurons in the neocortex. A subpopulation of interneurons expressing parvalbumin was also susceptible to this insult. We propose the mechanism mediating this effect is in part due to impaired VASP phosphorylation *via* partial inhibition of the CO/NO–sGC–cGMP pathway. CO exposure also results in behavioral changes in mice consistent with disrupted neocortical development.

2. Materials and methods

2.1. Animals and exposures

All animal work was approved by the USU IACUC. Timed pregnant mice (CD-1) were purchased from Charles River Laboratories (Wilmington, MA). Pregnant dams were housed individually in their cages within clear acrylic environmental chambers approximately 24″ × 24″ × 21″. Animals were provided with nestlets, food and water *ad libitum*. The chambers of all groups received an air flow of approximately 20 L/min. A CO concentration of 150 ppm was maintained in one chamber by mixing 7.5% CO with the carrier air flow and monitoring at least once per day (Interscan RM14-500M, Chatsworth, CA). This amount generates HbCO (carboxyhemoglobin) levels in the blood similar to those in a heavy smoker (10–16%). Smokers consume cigarettes to maintain a constant level of plasma nicotine (Henninfield and Goldberg, 1988). An average daily CO concentration for a typical experiment was 148 ± 3.8 (mean ± SEM) ppm. Dams displayed no behavioral changes during the exposure period and there was no mortality. See Supplemental Table 1 for effects of maternal CO exposure.

Our goal was to achieve the CO concentration of a person smoking one–two packs of cigarettes a day. Before finalizing on 150 ppm we attempted concentrations of 75 ppm and 500 ppm. We found that the lower concentration was not effective in achieving the required blood levels of HbCO (as seen in Supplemental Table 1). The higher concentration, however, produced behavioral changes in the pregnant mice that indicated toxicity. We therefore conducted our study using 150 ppm, which produced the desired blood levels and did not affect behavior, weight gain or rate of weight gain of the dams.

For *in vitro* experiments, slices were maintained in an incubator (95% O_2, 5% CO_2, 37 °C) at either 0 or 50 ppm CO. Exposure to 150 ppm was attempted in the organotypic slices, but at this exposure the cultures were not viable. Therefore, we reduced the concentration to 50 ppm. Migration was viable at 50 ppm and slices survived for the duration of the experiment. CO levels in the incubator were monitored with a GasBadge Pro CO detector (Industrial Scientific, Frederick, MD).

2.2. Histology and laminar measurements

For histologic and immunohistochemical experiments, mice were anesthetized using sodium pentobarbital solution (50 mg/kg), perfused with ice-cold phosphate buffered saline (PBS) followed by 4% paraformaldehyde in PBS. Brains were removed and stored in 4% paraformaldehyde at 4 °C; they were then sectioned, mounted, stained, and imaged within 72 h. We examined the somatosensory cortex in pups exposed to CO *in utero* at three ages: postnatal day 4 (P4), 11 (P11), or adult (P56 or later). 40 μm thick coronal sections from somatosensory cortex were stained with cresyl violet as previously described (Gittins and Harrison, 2004). At each age one pup from 4 different litters was chosen and 3 adjacent sections were evaluated. Images were taken using 10× magnification (Zeiss Axiovert 200, Thornwood, NY). The cortical thickness was measured as the distance from the pia to the white matter; the thickness of layers 1, 2–4, 5 and 6 was determined by cell morphology and density and measured using Axiovision software. Neuronal distributions and laminar measurements data were analyzed using a two-way ANOVA followed by a Holm–Sidak *post hoc* test for multiple comparisons (*e.g.*, Poluch et al., 2008).

2.3. Bromodeoxyuridine (BrdU) birthdating and Immunohistochemistry

For birth dating studies, 20 pregnant dams were injected 3× i.p. at 45 min intervals with bromodeoxyuridine (BrdU; 50 mg/kg, Sigma, St Louis MO) diluted in sterile saline on E12 or E16 as described previously (Miller and Nowakowski, 1988; Noctor et al., 1997; Wojtowicz and Kee, 2006; Duque and Rakic, 2011). Three injections were given due to the relatively short half-life of the compound and to maximize the quantity of labeled neurons born in a specific time period. Alternative groups of mice that did not receive BrdU were subjected to behavioral testing as described below. In all groups, animals were examined postnatally as adults (P56 or later). 40 μm thick vibratome prepared coronal sections were incubated overnight at 4 °C in either rabbit IgG antibodies against GAD 65/67 (1:500, Sigma), MAP2 (1:500, Sigma), CAMKIIα (1:200, Chemicon) or a mouse IgG antibody against parvalbumin diluted in buffer containing PBS, normal goat serum (NGS, 10%), and Triton X100 (0.3%). The slices were washed in PBS and incubated with appropriate secondary antibodies (Alexa Fluor 546-conjugated goat anti-rabbit or goat anti-mouse, 1:500). Slices containing somatosensory cortex were subsequently processed for BrdU immunohistochemistry as previously described (Poluch et al., 2008). Slices were incubated in ethanol (70%) for 10 min, then placed in 2 N HCl at 37 °C for 1 h, and rinsed in 0.1 borate buffer, pH 8.5 for 20 min. After washing in PBS, slices were incubated overnight at 4 °C in polyclonal rat IgG antibodies against BrdU (1:200; Accurate Chemical and Scientific Corp. Westbury, NY) in buffer containing PBS, NGS (10%), and Triton X-100 (0.3%). Slices were then washed in PBS, and then incubated for 3 h at room temperature with Alexa Fluor 488-conjugated goat anti-rat IgG (1:500). Slices were mounted onto slides using Mowiol, coded to a blind observer as to the treatment group, and coverslipped overnight prior to imaging. For analysis of each antibody or BrdU

immunoreactivity, at least 3 adjacent sections from 4 mice taken from 4 different litters were analyzed from treated and control groups. Also see Table 2.

2.4. Quantitative analysis of distribution

One person, who was blind as to treatment group, assessed the distrbution of labeled cells. To quantify the laminar distribution of double-labeled cells, we obtained images at 25× with an Axiovert 200 Zeiss microscope equipped with an Apotome and Axiovision 4.7. Images were transferred to Adobe Photoshop where 500 μm wide rectangles of somatosensory cortex approximately 2 mm lateral to the midline were selected and divided into 10 equal bins from the pia to the ventricular zone. The number of labeled cells in each bin was counted and plotted as a percent of the total number of labeled cells. Cells with dense staining of more than half the nucleus were considered BrdU-positive (Costa et al., 2001). Somatosensory cortex was chosen based on its well-characterized architecture and evidence of susceptibility to prenatal and perinatal insult (*e.g.*, Erzurumlu and Gaspar, 2012; Hara et al., 2012). Neuronal distributions and laminar measurements were analyzed using a two-way ANOVA followed by a Holm–Sidak *post hoc* test for multiple comparisons (*e.g.*, Poluch et al., 2008).

2.5. cGMP and VASP measurements

Brains from pups exposed to 0 or 150 ppm CO from E7 to P0 were rapidly removed at birth, flash frozen and stored at −80 °C. cGMP was extracted and measured using a commercially available ELISA kit according to the manufacturer's instructions (Cayman Chemical, Ann Arbor, MI). Proteins were extracted from whole brain as previously described (Jacobowitz and Heydorn, 1984) and subjected to Western blot analysis. Blots were probed for VASP and p-VASP (mouse anti-VASP, 1:1000; rabbit anti-phospho-VASP, 1:1000, Enzo Life Sciences, Plymouth Meeting, PA), subsequent secondary antibodies (anti-mouse, 1:5000; anti-rabbit, 1:5000, Li-Cor Biosciences, Lincoln, NE) and visualized using an Odyssey infrared imaging system (Li-Cor Biosciences, Lincoln, NE). Signal intensity from p-VASP band was divided by the intensity of VASP band to quantify the p-VASP to VASP ratio. cGMP levels, ratio of p-VASP-VASP and behavioral tests were compared between treated animals and controls using a Student's *t*-test.

2.6. Organotypic slice cultures

Embryos were taken from untreated CD-1 pregnant mice at E15 *via* cesarean section and their brains removed under sterile conditions in a laminar airflow hood. The brains were then cut into 350-μm thick coronal slices containing the ganglionic eminence (GE) and cortical plate using a tissue chopper (Stoeling, Wood Dale, IL). During dissection, brains and slices were perfused with cold oxygenated artificial cerebral spinal fluid (containing in mM: $CaCl_2$ 2.4, KCl 3.2, $MgSO_4$ 1.2, NaCl 124, $NaHCO_3$ 26, NaH_2PO_4 1.2, glucose 10). Slices were cultured on inserts (Millipore, Bedford, MA) and placed into 6-well plates in Neurobasal media (Gibco, Carlsbad, CA) containing B27, N2, and G.1.2 supplements. In six experiments, the phosphodiesterase inhibitor 3-isobutyl-1-methylxanthine (IBMX; 50 μM Sigma-Aldrich, St. Louis, MO) was added to the media. To visualize migrating neurons, we placed small crystals of DiI (1,1′-dioctadecyl-3,3,3′,3′-tetramethylindocarbocyanine perchlorate; Molecular Probes, Eugene, OR) into the GE. The slices incubated for 3 days at 95% O_2, 5% CO_2 at 37 °C with 0 or 50 ppm CO. Slices were then fixed overnight in a solution containing 4% paraformaldehyde in 0.1 M phosphate buffer (pH 7.4). Slices were incubated with the nuclear marker bisbenzamide (0.001%) for 10 min prior to imaging on a fluorescent microscope (Zeiss, Thornwood, NY).

2.7. Neuronal migration analyses

Migrating cells from the GE were assessed using a number of parameters. First, using Adobe Photoshop, borders were drawn to delineate between the cortical plate and the intermediate zone. The lateral border of interest was drawn at the corticostriate junction and the medial border drawn at the boundary of the cingulate cortex. We counted all DiI labeled cells between these boundaries that were contained in the intermediate zone or the cortical plate. The cortical plate was delineated as the dense cellular region approximately 300 μm wide as defined by staining with bisbenzimide. To determine the length of the leading process of a migrating cell, a line from the cell body to the tip of the leading process was measured using ImageJ. For cells with multiple branches, the lengths of all branches in a given cell were averaged (Poluch et al., 2008). Organotypic slice data were analyzed using a two-way ANOVA followed by a Holm–Sidak *post hoc* test for multiple comparisons (Poluch et al., 2008).

Table 1
The effects of prenatal CO on cortical wall and laminar thickness.

Age	0 ppm				150 ppm			
	Cortical thickness	Layer	Layer thickness (μm)	Layer proportion (%)	Cortical thickness	Layer	Layer thickness (μm)	Layer proportion (%)
P4	772 ± 20.1	I	47.1 ± 4.7	6.1 ± 0.7	*707.5 ± 38.7	I	38.6 ± 3.2	5.6 ± 0.3
		II–IV	200.7 ± 17.3	26.9 ± 3.2		II–IV	178.2 ± 11.5	24.9 ± 0.5
		V	220.5 ± 3.2	28.5 ± 1.5		V	232.2 ± 18.1	31.8 ± 0.3
		VI	277.7 ± 1.5	36.6 ± 1.8		VI	248.5 ± 19.4	37.2 ± 1
P11	782.6 ± 40.3	I	57 ± 2.9	7.9 ± 0.5	773.2 ± 17.8	I	56.3 ± 1.3	7.5 ± 0.1
		II–IV	263.7 ± 13.6	36.3 ± 2.1		II–IV	260 ± 6	34.6 ± 0.7
		V	225.6 ± 11.7	31.2 ± 1.8		V	223.8 ± 5.1	29.7 ± 0.6
		VI	235.3 ± 12.1	32.4 ± 1.9		VI	232.5 ± 5.3	30.8 ± 0.6
Adult	779.6 ± 21.1	I	89.4 ± 3.1	12.2 ± 0.3	787.2 ± 12.4	I	94.2 ± 1.9	12 ± 0.4
		II–IV	294.1 ± 10.2	40.1 ± 1		II–IV	309.9 ± 6.2	39.6 ± 1.2
		V	197.7 ± 6.8	27 ± 0.6		V	208.4 ± 4.1	26.6 ± 0.8
		VI	181.7 ± 6.3	24.8 ± 0.6		VI	191.4 ± 3.8	24.5 ± 0.8

Mice were exposed to 0 or 150 ppm in utero and examined at P4, P11, or as adults (P56 or later). The overall cortical thickness and laminar thicknesses were measured on cresyl violet stained sections of somatosensory cortex. Laminar thicknesses are also expressed as a percentage of total thickness for each section. Layers of neocortex are indicated with Roman numerals.
Data are mean ± SEM.
* $p < 0.05$, ANOVA, followed by Holm–Sidak *post hoc* test.

2.8. Behavioral tests

Adult mice exposed to 0 or 150 ppm CO *in utero* received a variety of behavioral tests during their active (dark) cycles. We measured locomotion using an Omnitech Electronics Digiscan infrared photocell system. Mice were placed in a 40 × 40 × 30 cm clear Plexiglas open field (OFT) and locomotion monitored for 1 h with an Omnitech Model DCM-I-BBU analyzer. The acoustic startle reflex and pre-pulse inhibition tests were measured in a Med Associates Acoustic Response Test System (St. Albans, VT). Startle stimuli consisted of 110 dB white noise bursts (20 ms) preceded 100 ms by 68, 79, or 90 dB 1 kHz pure tones (pre-pulse) (Paylor and Crawley, 1997). The hot plate responses were measured using an Omnitech Electronics Hot Plate Analgesiometer (Omnitech Electronics, Columbus, OH). Mice were placed on a 26 × 26 cm square platform maintained at 51 °C. Hotplate latencies were measured as the time from placement on the heated surface until the animal raised and licked a rear paw. Maximum time on the hotplate was 60 s. For behavioral tests, 1–2 pups were randomly selected from 4 litters (n = 7 for each treated and control group). Behavioral tests were compared between treated animals and controls using a Student's t-test.

We considered statistical significance to be reached at $p < 0.05$. Data summaries are expressed as mean ± standard error of the mean. Both male and female offspring were used in all parts of the study.

See Table 2 for the numbers of animals used in this study.

Table 2
Presented here are the numbers of litters and animals used in this study. These include the pregnant dams and the number of litters, as well as the offspring used in all aspects of the experiments. The number of litters are indicated in the top section; the number of pups or mice (*i.e.* those that matured and were used as adults) are shown on the bottom. For the animals used for Nissl and Immuno (E,F) 1 animal was used from 4 of the B & C litters for each different condition tested. For the animals used for organotypic cultures, 2 embryos from each litter were used to prepare the cultures. For the animals used in behavior (G), 1–2 animals from 4 of the A litters were used, while for the animals used for Biochemical experiments (H), 2 animals each from 4 of the A litters were used.

		Control	CO exposed*	Total
	Dams			
A	No inj	5 litters	7 litters	12 litters
B	BrdU inj E12	5 litters	5 litters	10 litters
C	BrdU inj E16	5 litters	5 litters	10 litters
D	organotypic	4 litters		4 litters
				36
	Pups/mice			
E	Nissl	12	12	24
F	Immuno	12	12	24
G	Behavior	7	7	14
H	Biochem	8	8	16
				78

* Does not include dams exposed to 75 ppm.

3. Results

3.1. Prenatal CO resulted in a thinner cerebral wall at P4

To determine if prenatal CO exposure resulted in gross anatomical changes, we examined the structure of somatosensory cortex in pups exposed to CO *in utero* at postnatal day 4 (P4), P11, and adult (P56 or later). Fig. 1 shows cresyl violet stained sections from untreated and CO exposed brains used to measure cortical thickness. At P4, CO treated mice had significantly thinner cerebral cortices compared to controls (707.5 ± 38.7 μm *vs* 772 ± 20.1 μm; $p < 0.05$). There were no significant differences in the relative size of each layer compared to the total cortical thickness (Table 1). CO treated mice recovered, showing no significant difference in overall cortical thickness or in cortical layers compared to controls at P11 and P56. This can be seen in the figures showing BrDU immunoreactivity.

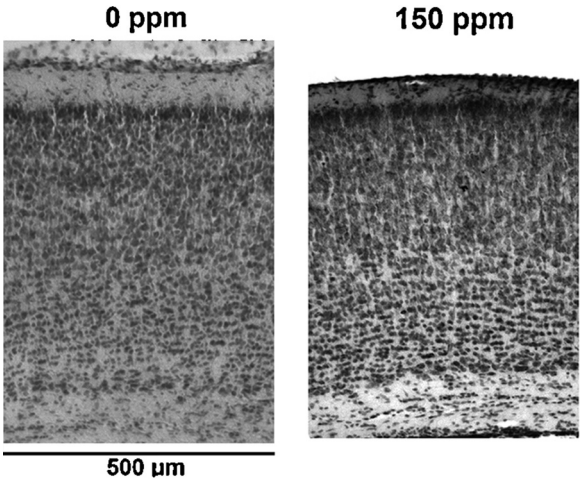

Fig. 1. Cresyl violet stained sections of somatosensory cortex at P4. Mouse pups were examined at P4, P11, or as adults (P56 or later), 40 μm thick coronal sections containing somatosensory cortex were stained with cresyl violet. Cortical thickness and layer thicknesses were measured in a region approximately 2 mm lateral to the midline. Shown here are images from a control (0 ppm) and treated (150 ppm) P4 somatosensory cortex. (n = 4 mice, 3 slices/mouse; * $p < 0.05$; Student's t-test). Also see Table 1.

3.2. Prenatal CO altered the distribution of cells born on E12 and E16

To determine if prenatal exposure to CO altered the laminar fate of neocortical cells, we examined the distribution of both early (E12) and later born (E16) cells using BrdU (Fig. 2). We chose these dates to best study effects on early and late corticogenesis. Four different mice from 4 different litters were used at each injection time; we assessed 3 sections from each mouse (*i.e.* a total of 12 sections). A high power view of immunoreactive cells can be seen in Fig. 2a, which also shows an image of the distribution of BrdU+ cells in a 500 μm wide column of cortex. In untreated mice, BrdU+ cells after injection at E12 distributed in the bins closer to the white matter, and predominantly located in bins 8–10 (Fig. 2d), as predicted from prior studies (*e.g.*, Price et al., 1997; Yozu et al., 2004). In CO exposed mice, a significant proportion of early born (E12) cells occurred in bin 7. After injections at E16, the BrdU+ cells in control brains located in bins 2 and 3, corresponding to layers 2 and 3 as expected (Fig. 2e). CO treated brains revealed that substantial BrdU+ cells were found in bins 4 and 5 (Fig. 2e).

3.3. Prenatal CO exposure did not alter the laminar organization of MAP2- or CAMKIIα-positive neurons

To determine the phenotype of displaced cells, we examined the distribution of cells likely to be projection neurons using antibodies targeting MAP2 or CAMKIIα (Fig. 3a; Supplemental Fig. 1) (Noctor et al., 1999; Curtetti et al., 2002). MAP2+ neurons distributed in all cortical layers, with higher numbers in bins 2 and 3, which correspond to layers 2/3 in untreated and CO-exposed adult cortex (Fig. 3b). Similar distributions of BrdU+ and MAP2+ cells were seen in control and CO-exposed mice (Fig. 3c and d). To confirm that likely projection neuron distributions did not alter after CO exposure, we also evaluated the distribution of CAMK-IIα+ cells, which are described as excitatory (*e.g.* Anderson et al., 2002). There was no significant difference in the distribution of CAMK-IIα+ cells in treated compared to control brains (Supplemental Fig. 1).

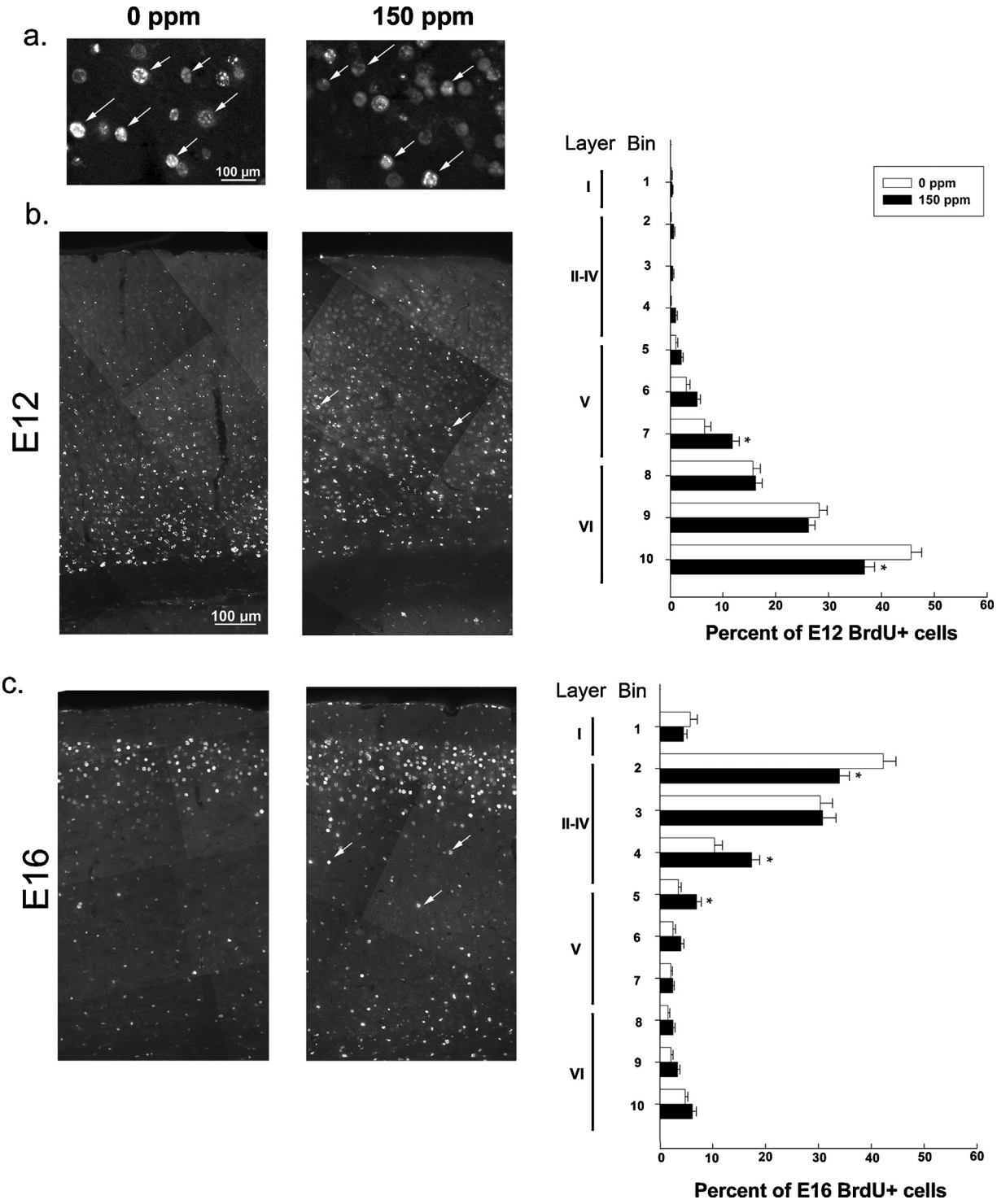

Fig. 2. Prenatal CO exposure results in displaced cells born on either E12 or E16. (a) Illustrates higher power views of BrdU immunoreactivity in the cortex of adult mice injected with BrdU *in utero* on E12 or E16. (b) And (c) show representative distributions of BrdU+ cells in the cortex of animals injected on E12 or E16. (d) And (e) show the quantified distributions of BrdU+ cells through the thickness of the cortex. The 500 μm wide region of cortex was divided into 10 equal bins. Bin 1 is adjacent to the pia and bin 10 adjacent to the white matter. BrdU+ cells were counted in each bin and plotted as a percent of the total number of BrdU+ cells. Prenatal CO exposure results in a significant proportion of displaced cells born either early (E12) or later (E16) during corticogenesis. In both cases, displaced cells were located toward middle layers of the cortex. The cortical layers corresponding to the bins are indicated with roman numerals in d and e. ($n = 4$ mice, 3 slices/mouse; $^{*}p < 0.05$; Two-way ANOVA, followed by Holm–Sidak *post hoc* test).

3.4. Prenatal CO altered interneuron distribution

Since the displaced neurons are not glutamatergic, we assessed whether they were GABAergic. To do so, we quantified the distribution of interneurons with the immunological marker GAD 65/67 in adult mice (Fig. 4a). There were no differences in the overall number of GAD65/67+ cells, but they showed differences in laminar positioning when comparing the untreated *versus* CO treated brains. Treated mice showed a laminar repositioning of interneurons with an increase in the proportion of interneurons in

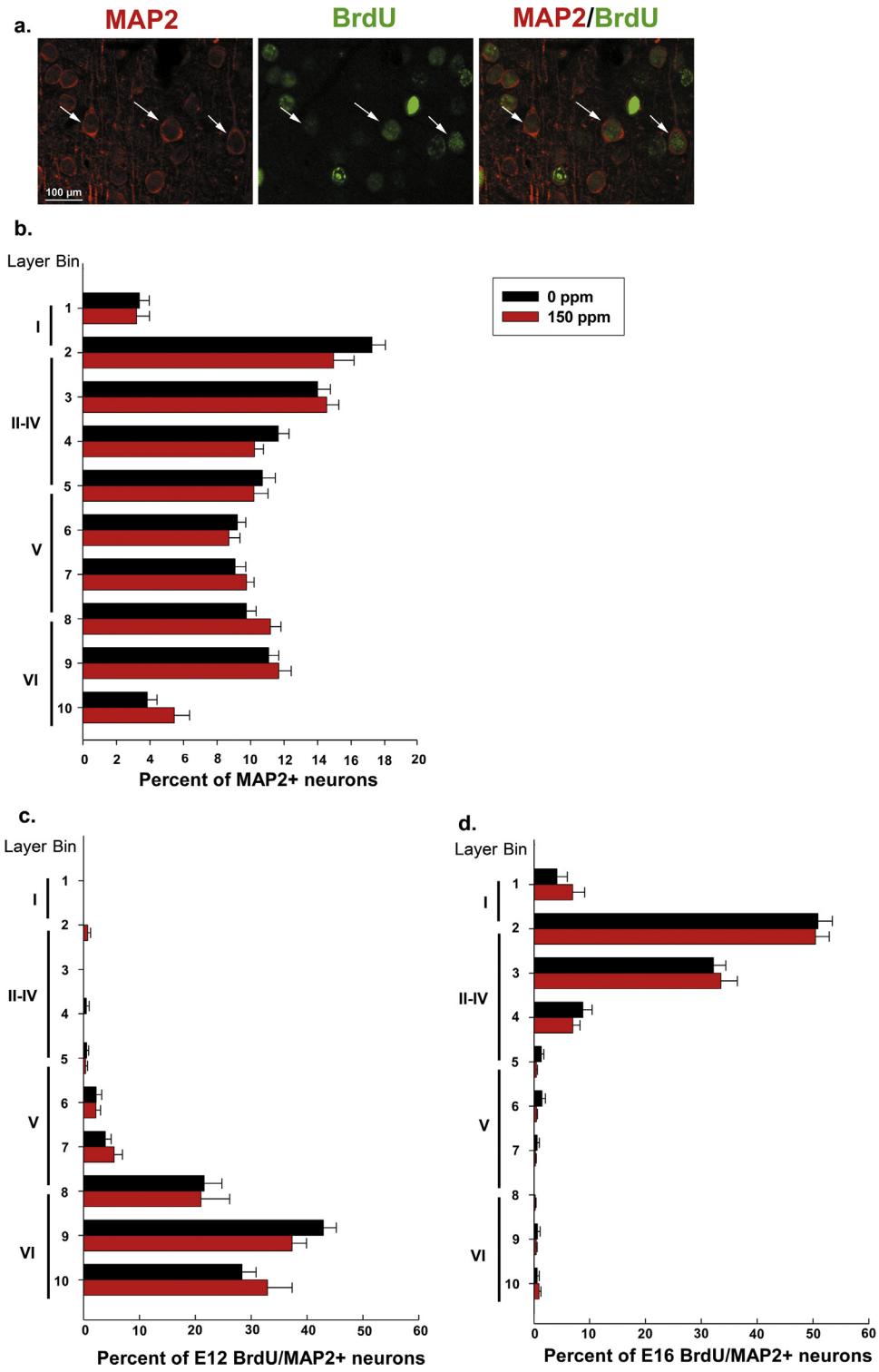

Fig. 3. Prenatal CO exposure does not affect the distribution of projection neurons. (a) Is an example of cells in the somatosensory cortex of mice immunoreactive for BrdU and MAP2. Arrows point to the same cells that are positive for MAP2, BrdU or both markers. (b) Shows the distribution of MAP2+ cells as a function of distance from the pia in equal sized bins through the thickness of the somatosensory cortex in control and CO treated cortex. Roman numerals designate approximate cortical layers. (c and d) Show the distribution of cells double labeled for MAP2 and BrdU when BrdU is injected on E12 (c) and when BrDU in injected on E16 injected (d). No significant differences between the control and CO-treated distributions are observed. (n = 4 mice, 3 slices/mouse).

upper layers (bin 3) and relative decrease in deeper layers (bin 7 and 8) of the cortex (Fig. 4b). We further investigated E12 and E16 born interneurons with BrdU immunohistochemistry. In treated adult mice, GAD65/67+ cells that incorporated BrdU on E12 were significantly displaced, showing an increase in bin 7 and a decrease in bins 9 and 10 (Fig. 4c). E16 BrdU+/GAD65/67+ cells were also significantly displaced, with an increase of proportion in bin 3 and 4 and a decrease in bin 2 (Fig. 4d). See Supplemental Fig. 2 for lower power images of BrdU and GAD65/67 immunohistochemistry.

To further determine if specific subsets of interneurons were affected by CO treatment, control and treated brains were immunoreacted with antibodies directed against parvalbumin

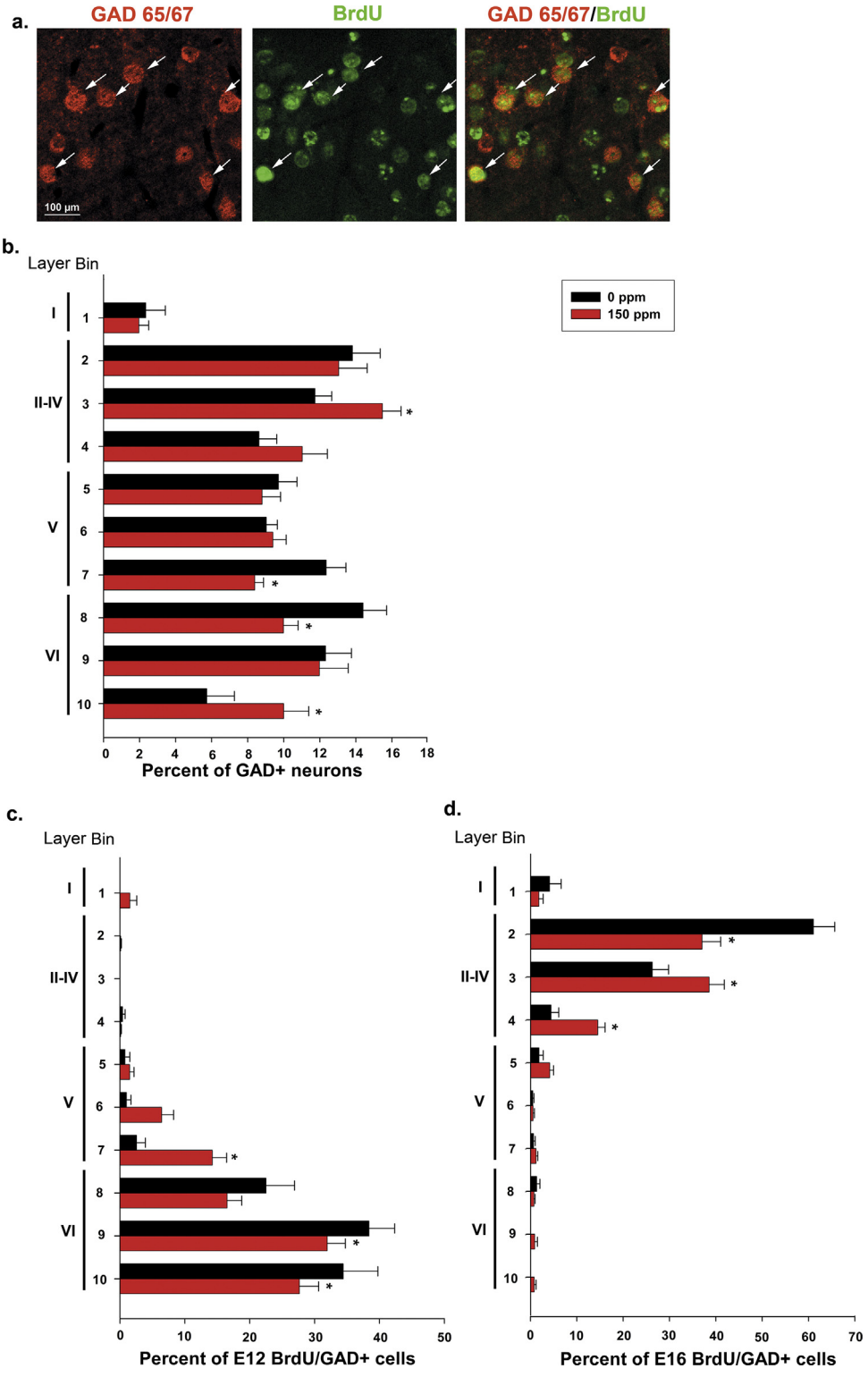

Fig. 4. Prenatal CO exposure affects the distribution of interneurons. (a) Is an example of cells in the somatosensory cortex of mice immunoreactive for BrdU and GAD 65/67 viewed at 25×. Arrows point to the same cells that are positive for both markers. (b) Shows the distribution of GAD 65/67+ cells as a function of distance from the pia in equal sized bins through the thickness of the somatosensory cortex in control and CO treated cortex. Roman numerals designate approximate cortical layers. (c and d) Show the distribution of cells double labeled for both GAD and BrdU when BrdU is injected on E12 (c) and when BrDU in injected on E16 (d). (n = 4 mice, 3 slices/mouse; $^{*}p < 0.05$; Two-way ANOVA, followed by Holm–Sidak *post hoc* test).

(PV; Supplemental Fig. 3). Subtle shifts occurred in the distributions of PV^{+} cells in the CO treated adult neocortex. In the overall pattern, PV+ cells were significantly increased in proportion in upper layer 2 (bin 2) and correspondingly decreased in lower layer 5 (bin 6) (Fig. 5a). PV+ cells born on E12 were almost entirely confined to layer 6 in control animals, but showed a dramatic increase in layer 5 in CO treated adult mice (bin 7, Fig. 5b). E16 born PV+ cells were proportionally reduced in bin 2 in treated mice (Fig. 5c). See Supplemental Fig. 3 for a lower power view of BrdU coupled with PV immunohistochemistry. Since cortical GABAergic

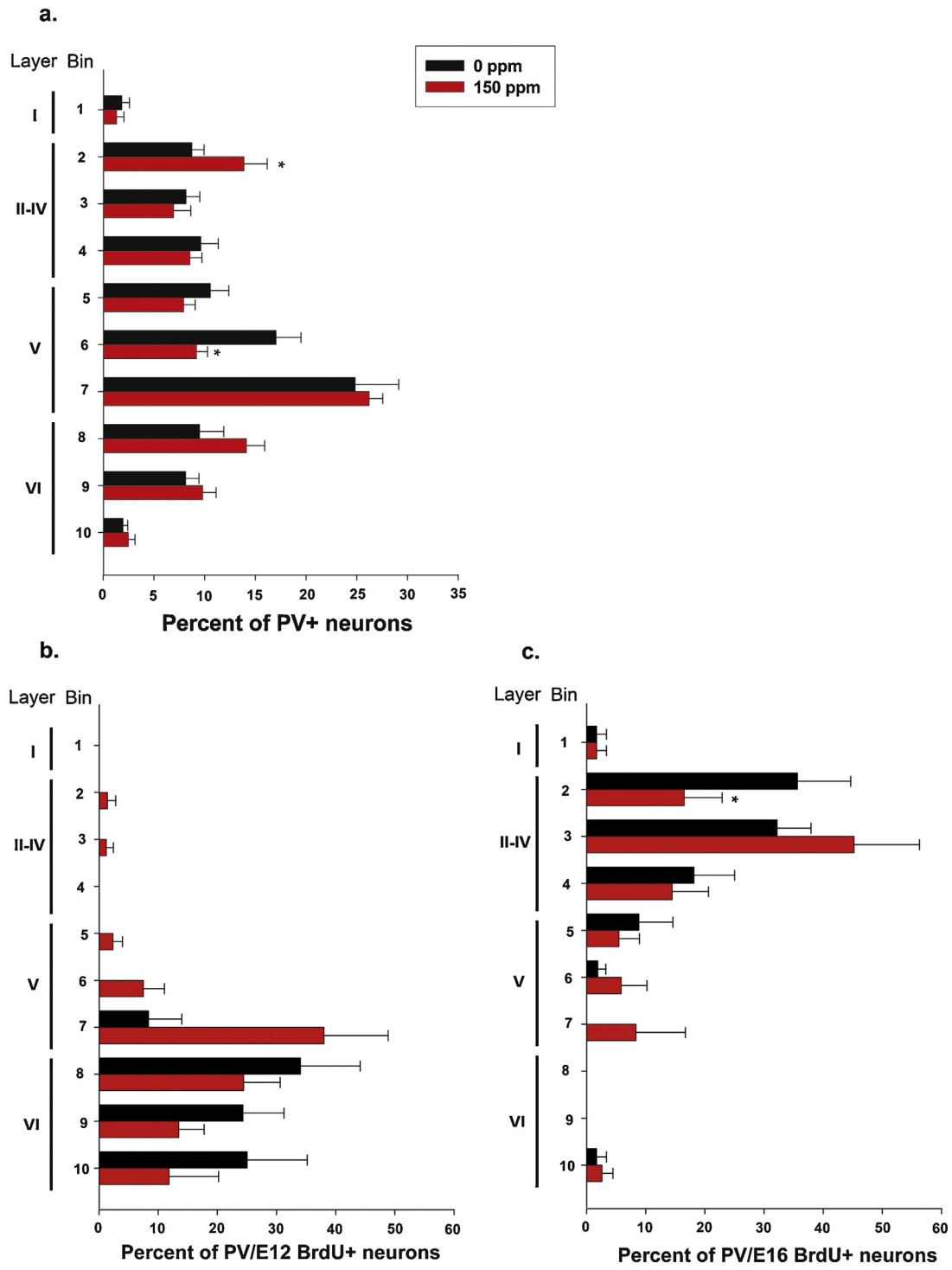

Fig. 5. Prenatal CO exposure affects the distribution of PV^+ interneurons. (a) Shows the distribution of PV+ cells as a function of distance from the pia in equal sized bins through the thickness of the somatosensory cortex in control and CO treated cortex. Roman numerals designate approximate cortical layers. (b and c) Show the distribution of cells labeled for both PV and BrdU when BrDU is injected on E12 (b) and when BrDU in injected on E16 (c). ($n = 4$ mice, 3 slices/mouse; $^* p < 0.05$; Two-way ANOVA, followed by Holm–Sidak *post hoc* test).

neurons are born in the ganlgionic eminence and reach the cortex *via* tangential migration, our results suggest that this process is altered in animals exposed to CO in utero.

3.5. CO exposure impairs interneuron migration and results in shorter leading processes

To study the direct effects of CO gaseous signaling on interneuron migration we used organotypic slices. Cells in the ganglionic eminence were labeled using DiI (Fig. 6). After 3 days *in vitro*, the slices were placed in fixative prior to imaging. To determine factors that might affect the motility of migrating cells after exposure to CO, we measured the length of the leading processes. In control conditions, the mean leading process length was 78.4 ± 0.7 μm (Figs. 6C and Fig. 7). Treated cells had significantly shorter leading processes (64.3 ± 1.3 μm; $p < 0.001$; Figs. 6E and Fig. 7), suggesting that the ability to migrate effectively was altered. This was true both for measurements while cells

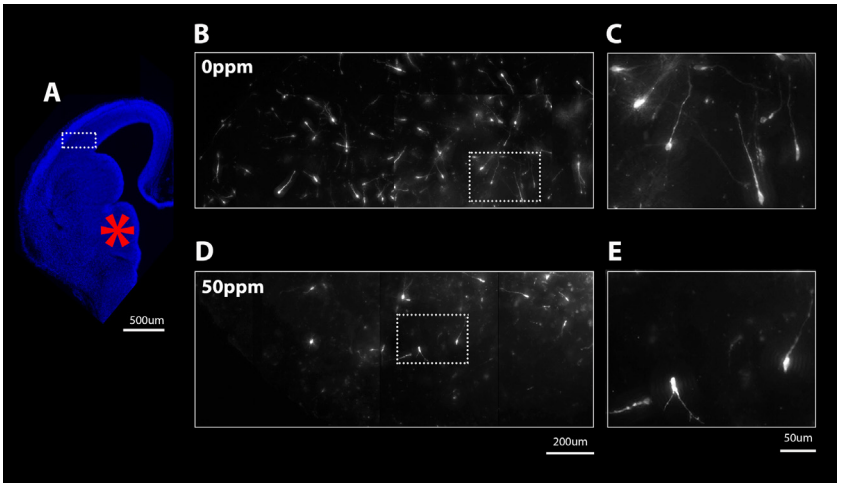

Fig. 6. DiI labels migrating interneurons in E15 organotypic slices. On the left is an example of an organotypic slice with the position of the DiI crystals in the medial ganglionic eminence. Slices were maintained for 3 days in an incubator with administration of either 0 or 50 ppm CO. The top middle panel shows cells migrating in the intermediate zone with no CO treatment (0 ppm) and (C) is a higher power view of the boxed in region. (D) shows cells migrating in the intermediate zone after treatment with 50 ppm CO and (E) is a higher power view of individual migrating cells. These cells exhibit a distinct leading process, which also have multiple branches that explore the extracellular environment. The leading processes were shorter in the slices treated with 50 ppm CO. Dorsal is up, medial is to the right, and lateral is to the left.

migrated in the intermediate zone, as well as those that reached the cortical plate.

3.6. Prenatal exposure to CO results in decreased levels of cGMP and phospho-VASP

To better understand an underlying mechanism that might influence impaired migration, we determined if CO exposure affected production of the secondary messenger cGMP. Brains of pups (P0) from 2 different litters were assayed for cGMP after exposure to either 0 or 150 ppm CO from E7 until birth. Exposed mice had significantly lower levels of cGMP (Fig. 8a). To determine if downstream targets of cGMP were affected, brains from alternate pups were assayed for proteins using Western blots. We probed for p-VASP and VASP in the same blot, and imaged the bands simultaneously on different infrared emission channels (Fig. 8b). The phosphorylated form of VASP should inform if VASP has been activated downstream of cGMP. From those images, we quantified the ratio of p-VASP to VASP. Mice exposed to CO *in utero* had significantly lower p-VASP/VASP ratios (Fig. 8c) suggesting less activation of VASP.

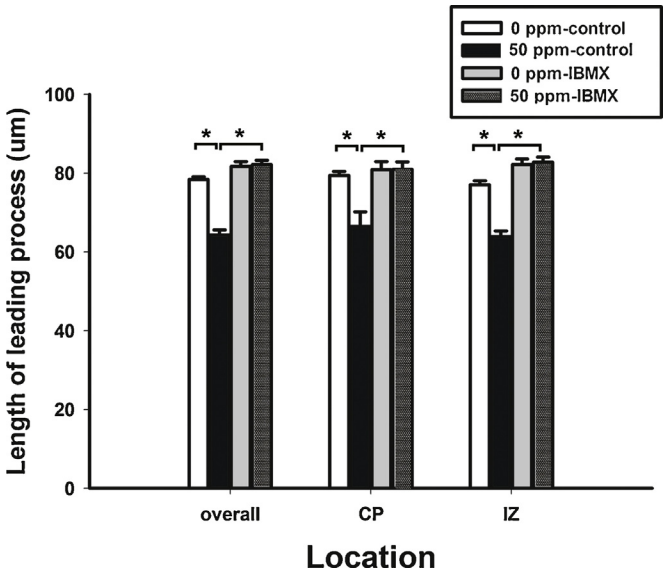

Fig. 7. CO exposure results in shorter leading process of migrating cells; the effect is reversed by IBMX. Organotypic slices containing DiI injections into the medial ganglionic eminence were grown in 0 or 50 ppm CO. After 3 days in culture, the length of the leading process of migrating interneurons was measured as described in the Methods. In control slices migrating interneurons had an average leading process length of 78.4 ± 0.7 μm throughout the developing cortex. This was consistent in the cortical plate (CP) and intermediate zone (IZ). In slices treated with 50 ppm CO cells had significantly shorter leading processes compared with the control lengths (64.3 ± 1.3 μm). This effect was completely reversed by the phosphodiesterase inhibitor IBMX (50 μm) where the migrating cells of CO treated cultures showed no differences in leading process length compared with untreated controls ($n = 5$ slices/group; $p < 0.05$, Two-way ANOVA followed by Holm–Sidak *post hoc* test).

3.7. IBMX restored the leading processes of migrating interneurons

Since CO ultimately impaired neuronal migration and the treated cells had shorter leading processes, we asked if the CO/NO–cGMP–cGK pathway was affected, as suggested by the cGMP reduction in CO treated brains. CO can act as a partial agonist to sGC, however, in our experiment, chronic exposure resulted in the decrease of cGMP. To maintain endogenously produced cGMP, we used the phosphodiesterase inhibitor IBMX. We then measured the length of leading processes in cells treated with IBMX and grown in the presence of CO. In CO treated slices, IBMX successfully restored the length of leading processes of migrating interneurons (Fig. 7). This effect was valid for cells reaching the cortical plate and those found in the intermediate zone.

3.8. Prenatal exposure to CO produced changes in animal behavior

To determine if CO exposure had long lasting impacts on cortical function, we explored behavior in adult mice using three behavioral paradigms: the OFT, pre-pulse inhibition test, and hot plate test. In overall locomotor behavior, the treated mice appeared remarkably similar to controls. When assessed in the open field, treated mice behaved similar to controls in a variety of parameters including overall activity, distance traveled and time spent moving (Fig. 9a). Mice were tested for sensorimotor gating using the pre-pulse inhibition test. Control mice reliably inhibited their response by approximately 20%; however treated mice did not possess significant pre-pulse inhibition and consistently reacted strongly to the startle stimulus (Fig. 9b). In the hot plate test, control mice

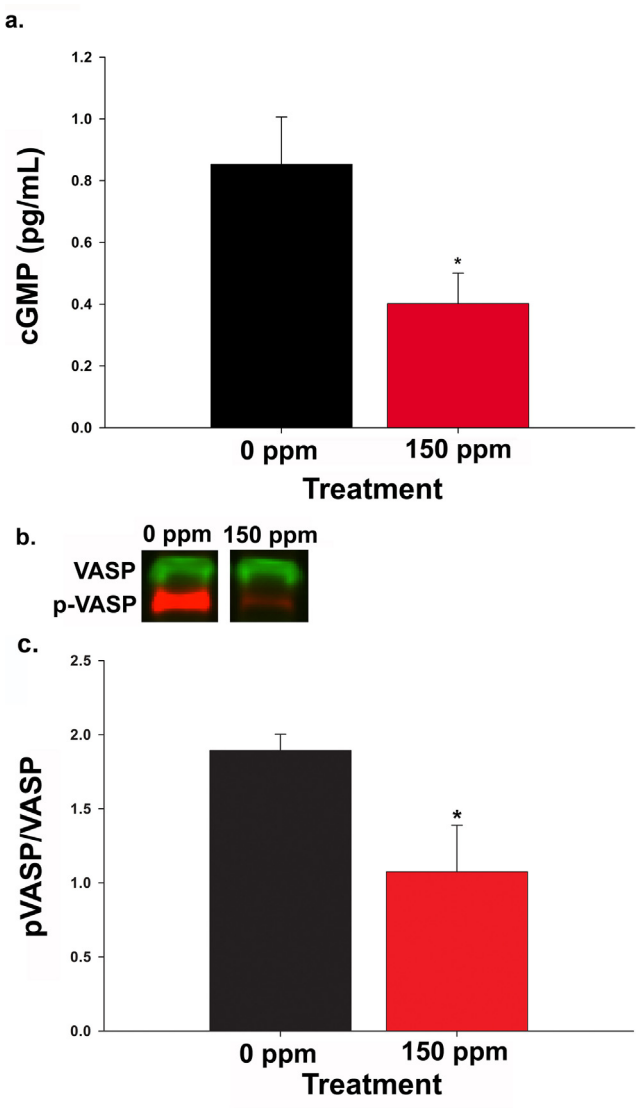

Fig. 8. Prenatal CO exposure results in a decrease in cGMP and phosphorylated VASP. Pregnant dams were exposed to 0 or 150 ppm CO from E7 until birth. (a) Indicates cGMP levels in treated *vs.* control mice. CO treated pups (P0) had significantly reduced cGMP levels compared to controls (0.4 ± 0.1 *vs.* 0.85 ± 0.153 pg/mL; $n = 5$, $p < 0.05$, Student's *t*-test). (b) Shows a western blot of both phospho-VASP and VASP (green). (c) Shows the quantification of the western blot. CO treated pups had significantly reduced phospho-VASP/VASP ratios compared to controls (1.1 ± 0.3 *vs.* 1.8 ± 0.1; $n = 5$, $p < 0.05$, Student's *t*-test). Pups taken from two different litters were used for this assay.

elicited a paw withdrawal response latency of 32.7 ± 1.8 s. Treated mice had significantly lower nociceptive thresholds, with a mean response of 22.6 ± 1.5 s (Fig. 9c). These results suggest that negative behavioral responses to CO exposure in utero persist into adulthood.

4. Discussion

The results of our study show changes in both structure and function of the cerebral cortex after prenatal CO exposure. Exposure to low concentrations of CO during neocortical development, similar to the amount inhaled by heavy smokers, results in an altered laminar fate of cells. The majority of displaced cells are interneurons. Mice exposed to CO *in utero* also lack pre-pulse inhibition to the acoustic startle reflex and are significantly hyperalgesic. We thus demonstrate here another toxic effect of

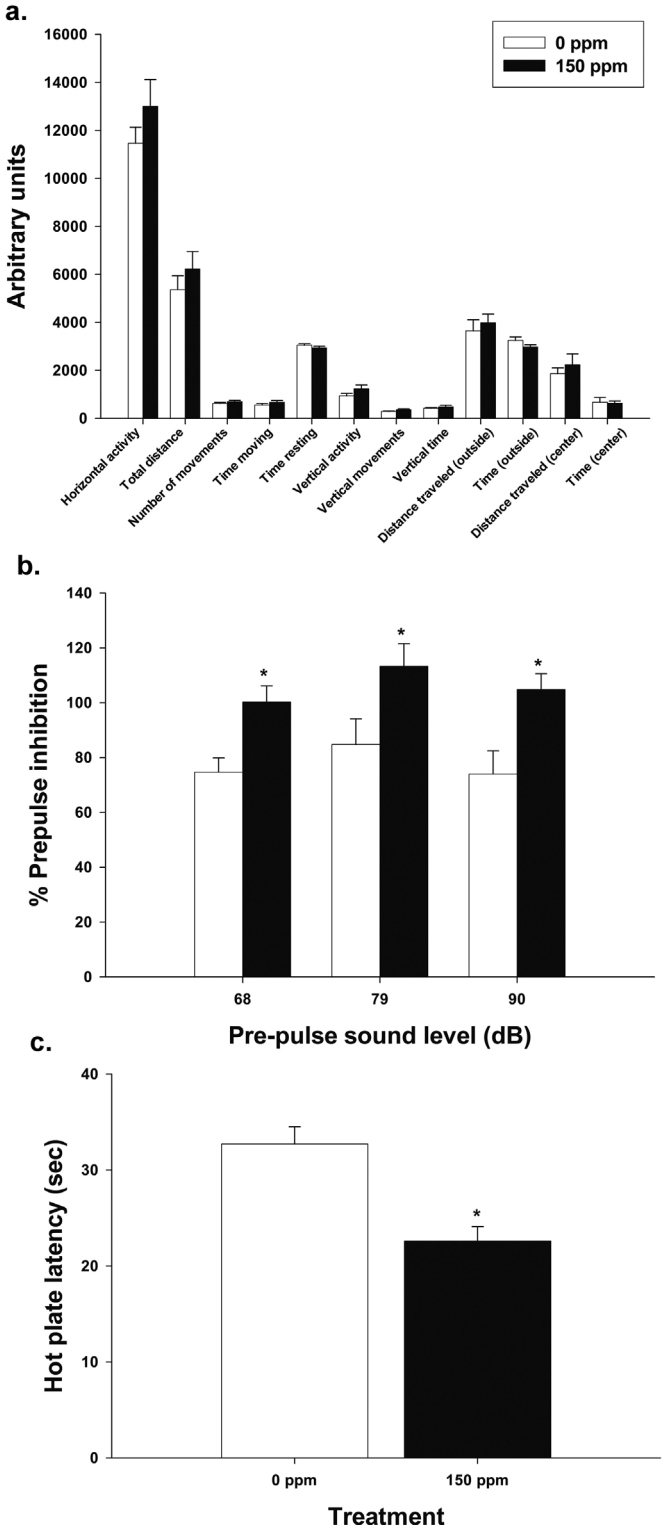

Fig. 9. Prenatal CO results in functional deficits in adult mice exposed *in utero*. (a) Shows graphic summary of analysis of parameters evaluated with the open field test. Open bars demonstrate the means of control animal responses and filled bars show the means of CO treated animals. (b) Displays a graphic summary of the pre-pulse inhibition test, as a percent of startle response without pre-pulse, as a function of strength of the pre-pulse sound. (c) Hot plate test, shows mean time elapsed from being placed on the hot plate to foot lick ($n = 7$, * $p < 0.05$, Student's *t*-test).

maternal smoking that can produce permanent structural and functional consequences in the developing fetus.

Prenatal exposure to CO produces a number of neurological effects. When delivered at low concentrations, CO induces a variety

of neurobehavioral abnormalities in rat offspring (Fechter and Annau, 1977, 1980; Mactutus and Fechter, 1984, 1985; Di Giovanni et al., 1993). Prenatal CO exposure also affects a variety of neurotransmitters in the developing brain. Cagiano et al. (1998) demonstrated in male rats that low CO concentrations elicited changes in mesolimbic dopaminergic function and impaired sexual behavior. Storm and Fechter (1985) found changes in cerebellar catecholamines and linked these changes with deficiencies in motor test performance and in learning and memory. Storm et al. (1986) noted a decrease in total GABA content in the cerebelli of 10 day old rats exposed to CO prenatally, suggesting GABAergic neurons may represent a subpopulation of neurons particularly vulnerable to CO toxicity. Later, Benagiano et al. (2005) demonstrated layer specific decreases in GABA content in the cerebellum, to support evidence of motor impairments. We demonstrate altered laminar fate and distribution of interneurons in adults exposed to CO during fetal development. Our study and others (Benagiano et al., 2005) suggest that GABAergic neurons may represent a subpopulation of neurons particularly vulnerable to CO toxicity. This is significant considering that GABA signaling is often altered in neurological disorders such as schizophrenia (Hyde et al., 2011; Tao et al., 2012).

It may be tempting to ascribe the results observed to acute or chronic hypoxia. Studies of acute hypoxia, however, use low levels of O_2 *in vivo* or *in vitro*. Those levels are not sustainable by animals or humans for any length of time. These studies use PO_2 levels in the range of 30 mmHg and hemoglobin O_2 saturations of 50–60%. We measured blood levels in some dams at the end of exposure ($\sim$14 days of exposure) and never measured an O_2 saturation below 80% in the 150 ppm group (carboxyhemoglobin $<$ 20%). While we cannot discount the possibility that hypoxia played some role in the changes we measured, the HbCOs are in the range of a heavy smoker, not someone acutely or chronically hypoxic.

4.1. CO administration during neocortical development alters interneuron distribution

In our *in vitro* study the leading processes of CO treated cells were significantly shorter. This suggests that the laminar defect observed in treated adults is the result of altered tangential migration of GABAergic neurons generated in the ganglionic eminence. Interestingly the normal distribution of MAP2 and CAMK-IIα projection neurons indicates selective vulnerability to insult during development. Previous work in our lab reported this cell population as uniquely susceptible to environmental insults (Poluch et al., 2008). Specific involvement of GABAergic neurons has also been noted in other models of maternal exposure including cocaine (Crandall et al., 2004; McCarthy et al., 2011), bisphenol (Nakamura et al., 2007), ethanol (Cuzon et al., 2008) and methylazoxy methanol (Poluch et al., 2008). One possibility to selectively affect GABAergic cells is the well-known long and arduous path of migration taken by interneurons, which may make them more susceptible to disruptions (*e.g.*, Wonders and Anderson, 2006). We observed alterations of a subpopulation of interneurons: PV-expressing cells. PV expressing interneurons arise from the medial ganglionic eminence MGE and represent a unique subpopulation of interneurons based on morphology and activity (*e.g.* Inan et al., 2012). They reside predominantly in middle to deeper layers of the cortex, have a distinctive basket-like morphology, and generally show fast-spiking firing activity (Kawaguchi and Kondo, 2002). These displaced PV cells may alter the overall excitatory/inhibitory tone throughout the cortex. In addition, the leading processes of treated cells were significantly shorter, suggesting that CO treatment affected cytoskeletal components. This supports previous research implicating the importance of the cytoskeletin influencing the rate of cellular migration (Goh et al., 2002).

4.2. The CO/NO–cGMP pathway is important for neuronal migration

The developing fetus is particularly vulnerable to insult, as CO readily crosses the placenta and binds to fetal hemoglobin with a higher affinity than adult hemoglobin (Longo, 1970). During chronic exposure, the gas may accumulate in tissues and act as a signaling molecule. CO and NO participate in many similar signaling pathways. NO is important for cellular processes involved in development and neuronal migration, particularly through the formation of the second messenger cGMP (Haase and Bicker, 2003). The role of NO-mediated production of cGMP through the activation of soluble guanylate cyclase (sGC) in neuronal migration was characterized in detail using insect models of development. In the hemimetabolous grasshopper (*Locusta migratoria*), Haase and Bicker (2003) observed that NO-induced production of cGMP is an essential component of neuronal migration in that neurons fated for the midgut plexus exhibited inducible cGMP immunoreactivity during the migratory phase of development. Furthermore, pharmacologic inhibition of endogenous nitric oxide synthase (NOS), sGC, and cGMP-dependent kinase (cGK) each significantly decreased neuronal migration (Haase and Bicker, 2003). Endogenous CO is produced by heme oxygenase (HO) *via* the metabolism of heme, and can signal comparably to NO *via* the cGMP/cGK cascade (Boehning et al., 2003). In the grasshopper embryo, enteric neurons express HO while migrating to the midgut, suggesting CO may also play a critical role in migration (Bicker, 2007). In an *in vitro* model Tegenge and Bicker (2009) showed that NO and cGMP positively induce neuronal migration in human neuronal precursor (NT2) cells. Ding et al. (2005) described the developmental expression profile of sGC in the mouse, which parallels the period of neuronal migration in the developing brain. Furthermore, mice with the gene for sGC deleted develop an abnormal neocortex, consistent with deficiencies in neuronal migration (Demyanenko et al., 2005). In the mouse embryo, tangentially migrating neurons from the ganglionic eminence produce cGMP earlier than neurons situated in the cortex, and also produce cGMP in response to exogenous NO treatment (Currie et al., 2006). The evidence that cGMP is crucially involved in neuronal migration suggests that alterations of cGMP levels, such as that induced by exogenous CO, may dramatically affect neuronal migration and neocortical development.

Because previous studies demonstrated the effects of NO on neuronal migration, we hypothesized that CO could influence migration by affecting the production of cGMP. Under normal conditions, NO stimulates soluble gunaylate cyclase to produce cGMP. cGMP then activates a cGMP-dependant kinase, which phosphorylates a number of important proteins, including the actin associated protein VASP. Phosphorylation of VASP prevents the capping of actin, and promotes polymerization, a critical component of neuronal migration (Fig. 10a). CO acts as an agonist to soluble gunanylate cyclase similar to NO, and can also result in the formation of cGMP (Verma et al., 1993). Our early expectation was that CO exposure would result in an increase in cGMP. However, chronic CO exposure *in utero* resulted in a cGMP decrease in pups at birth. Furthermore, although CO activates sGC with a similar mechanism to NO, it activates sGC 25–50 fold less than NO (Kharitonov et al., 1995) Therefore, CO appears to act as a partial agonist to the enzyme during chronic exposure, thereby interfering with the formation of cGMP by endogenous NO (Fig. 10b).

Decreased cGMP leads to a decrease in the subsequent activation of cGMP dependent kinases, which phosphorylate a number of proteins involved in neuronal migration such as the actin associated complex Ena/VASP. Under normal conditions, phosphorylation of Ena/VASP results in actin binding, preventing

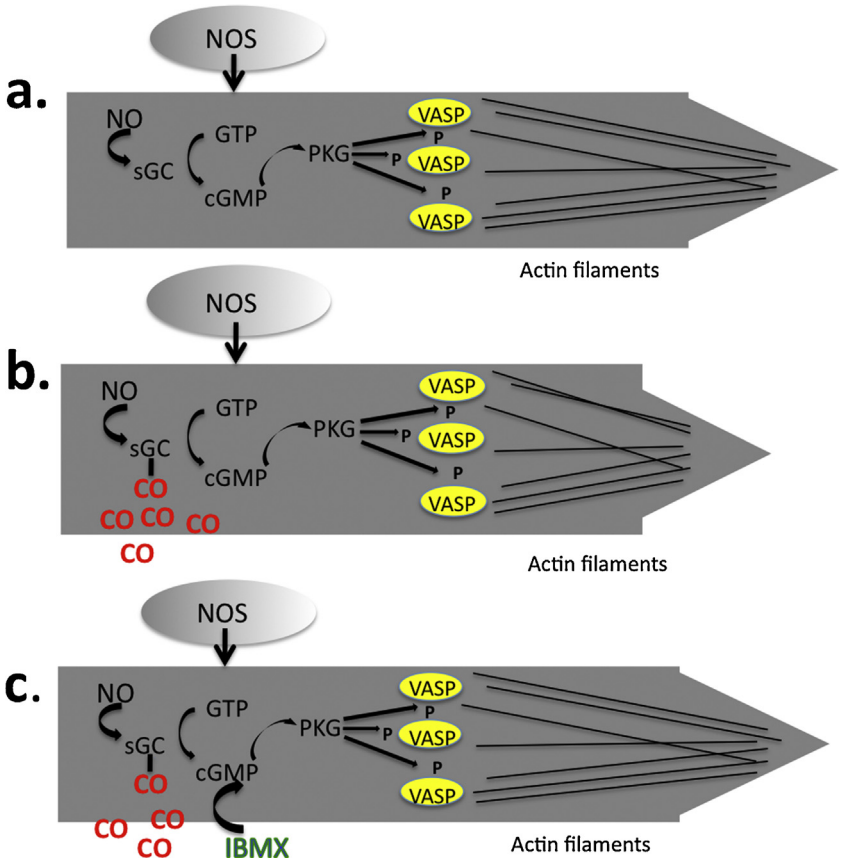

Fig. 10. Model of the effects of NO and CO on neuronal migration. (a) Shows that NO stimulates soluble guanylate cyclase (sGC) to produce cGMP. cGMP then activates a cGMP dependent kinase to phosphorylate VASP. Phospho-VASP inhibits the capping of actin, and promotes polymerization, which leads to leading process extension and neuronal migration. (b) CO acts as a partial agonist to soluble guanylate cyclase (sGC), and in the chronic exposure results in a decrease in cGMP. This leads to decreased phospho-VASP, shortened leading processes, and diminished neuronal migration. (c) Shows that inhibition of phosphodiesterase with IBMX can partially rescue the effect of CO on both leading process length and neuronal migration.
Abbreviations—NO: nitric oxide; cGMP: cyclic-guanosine monophosphate; VASP: vasodialator-stimulated phosphoprotein; CO: carbon monoxide; IBMX: 3-isobutyl-1-methylxanthine.

the binding of other capping proteins. This results in the continued polymerization of actin, a critical element in neuronal migration (Laurent et al., 1999). To illustrate the importance of Ena/VASP during neuronal migration and development, Goh et al. (2002) disabled Ena/VASP through the retroviral introduction of FP4-MITO, which binds Ena/VASP to mitochondria. This resulted in a shift of layer 5 pyramidal neurons to upper layers 2 & 3 of the cortex. The authors attributed this effect to either a delayed emergence from the ventricular zone or a decreased rate in migration. We show here that chronic exposure to CO results in a decrease in phospho-VASP. These decreased levels may also have effects on neuronal migration, specifically interneurons migrating from the GE.

4.3. Migration defects caused by CO are reversed by IBMX

An additional goal of this study was to determine if CO impaired migration *via* cGMP dependent pathways. If CO acts as a partial agonist to sGC, then it may be possible to maintain the cGMP produced by inhibiting its breakdown. To test this hypothesis we incubated organotypic slices in both control and CO environments in the presence of the phosphodiesterase inhibitor IBMX. In CO treated slices, IBMX treatment resulted in a complete recovery in the length of leading processes, suggesting that cGMP levels were a critical component to the cytoskeletal architecture involved in cellular migration (Fig. 10c). These data further support our hypothesis that CO impairs migration of cells *via* the inhibition of cGMP production.

4.4. CO directly affects migrating interneurons as a signaling molecule

Our results have profound implications in understanding CO toxicity, particularly in chronic low levels. Chronic exposure may result in an increased cellular partial pressure of CO and have effects on NO-mediated signaling pathways. As indicated above, although CO can activate sGC with a mechanism similar to NO, it does so with greatly reduced rate. Here we demonstrate that chronic CO exposure results in a decrease in cGMP and phospho-VASP. This effect is rescued with the phosphodiesterase inhibitor IBMX, which causes recovery in the length of leading processes of migrating neurons. These data provide further evidence of the toxic effect of chronic low level CO exposure on brain development. Our organotypic slice experiments demonstrate that CO can impair migration *via* the CO–sGC–cGMP pathway. This effect is merely one of many mechanisms mediating the toxicity of CO. CO also affects oxidative metabolism *via* inhibition of cytochromes in the mitochondrial electron transport chain. A recent study by Cheng et al. (2012) showed that brief perinatal exposure to 100 ppm CO impairs cytochrome c release, caspase-3 activation, and inhibits developmental apoptosis (Cheng et al., 2012). While this study demonstrates an additional mechanism that could account, in part, for our results, its brief exposure (3 h) during the perinatal period is

a major difference in study design, making it difficult to directly compare the results.

4.5. CO administration during neocortical development leads to alterations in behavior

Prenatal CO exposure also resulted in behavioral changes of the offspring. Overall locomotor activity was similar in treated mice compared to controls. This was not surprising, as the differences noted in interneuron distribution were subtle, and not detected with a gross behavioral test. The pre-pulse inhibition test measures sensorimotor gating more sensitively, which engages many brain structures, including somatosensory, insular, and cingulate cortices (Neuner et al., 2010). This test is highly conserved across mammals, and considered one of the most translatable tests from mouse to human (Crawley et al., 1997). Mice exposed to CO *in utero* showed impaired pre-pulse inhibition. This phenomenon occurs in schizophrenic patients, who also have altered interneuron distribution and lack pre-pulse inhibition (Braff et al., 1978; Kumari et al., 2000). The hot plate test assesses supraspinal mediated pain processing that involves somatosensory cortex and GABAergic transmission. Transgenic mice lacking GAD-65 demonstrated hyperalgesia, while mice bred to overexpress the GABA transporter GAT-1, altering the tonic GABA levels in the synaptic environment, exhibited hyperalgesia to a variety of thermal and chemical nociceptive challenges (Hu et al., 2003). In our study, mice exposed to CO *in utero* had significantly shorter hot plate latencies compared to controls, consistent with previous reports that alterations in GABAergic activity can influence nociception. Overall, these observations suggest that the alterations we found in neocortical cell positioning and impaired migration were reflected in behavior.

Conflict of interest statement

None declared.

Acknowledgements

The authors would like to thank Dr. Neil Grunberg and the members of his laboratory for allowing us to use their behavioral testing equipment, and LaToya Hyson for her technical expertise and assistance with experiments. We would also like to thank Dr. Ajay Verma for his inspiration and support. This work was funded by the Flight Attendant's Medical Research Institute (FAMRI 072226 CIA) and through USU R086IN intramural grant and PHS RO1 NS24014.

Appendix A. Supplementary data

Supplementary material related to this article can be found, in the online version, at http://dx.doi.org/10.1016/j.neuro.2015.11.002.

References

Algan, O., Rakic, P., 1997. Radiation-induced, lamina-specific deletion of neurons in the primate visual cortex. J. Comp. Neurol. 381, 335–352.
Ang Jr., E.S., Gluncic, V., Duque, A., Schafer, M.E., Rakic, P., 2006. Prenatal exposure to ultrasound waves impacts neuronal migration in mice. PNAS 103, 12903–12910.
Anderson, S.A., Kaznowski, C.E., Horn, C., Rubenstein, J.L., McConnell, S.K., 2002. Distinct origins of neocortical projection neurons and interneurons in vivo. Cereb. Cortex 12, 702–709.
Benagiano, V., Lorusso, L., Coluccia, A., Tarullo, A., Flace, P., Girolamo, F., Bosco, L., Cagiano, R., Ambrosi, G., 2005. Glutamic acid decarboxylase and GABA immunoreactivities in the cerebellar cortex of adult rat after prenatal exposure to a low concentration of carbon monoxide. Neuroscience 135, 897–905.
Bicker, G., 2007. Pharmacological approaches to nitric oxide signalling during neural development of locusts and other model insects. Arch. Insect Biochem. Physiol. 64, 43–58.
Boehning, D., Moon, C., Sharma, S., Hurt, K.J., Hester, L.D., Ronnett, G.V., Shugar, D., Snyder, S.H., 2003. Carbon monoxide neurotransmission activated by CK2 phosphorylation of heme oxygenase-2. Neuron 40, 129–137.
Braff, D., Stone, C., Callaway, E., Geyer, M., Glick, I., Bali, L., 1978. Prestimulus effects on human startle reflex in normals and schizophrenics. Psychophysiology 15, 339–343.
Cagiano, R., Ancona, D., Cassano, T., Tattoli, M., Trabace, L., Cuomo, V., 1998. Effects of prenatal exposure to low concentrations of carbon monoxide on sexual behaviour and mesolimbic dopaminergic function in rat offspring. Br. J. Pharmacol. 125, 909–915.
Caughey, W.S., 1970. Carbon monoxide bonding in hemeproteins. Ann. N. Y. Acad. Sci. 174, 148–153.
Cheng, Y., Thomas, A., Mardini, F., Bianchi, S.L., Tang, J.X., Peng, J., Wei, H., Eckenhoff, M.F., Eckenhoff, R.G., Levy, R.J., 2012. Neurodevelopmental consequences of sub-clinical carbon monoxide exposure in newborn mice. PLoS ONE 7, e32029.
Choi, B.H., Lapham, L.W., Amin-Zaki, L., Saleem, T., 1978. Abnormal neuronal migration, deranged cerebral cortical organization, and diffuse white matter astrocytosis of human fetal brain: a major effect of methylmercury poisoning in utero. J. Neuropathol. Exp. Neurol. 37, 719–733.
Costa, C., Harding, B., Copp, A.J., 2001. Neuronal migration defects in the Dreher (Lmx1a) mutant mouse: role of disorders of the glial limiting membrane. Cereb. Cortex 11, 498–505.
Crandall, J.E., Hackett, H.E., Tobet, S.A., Kosofsky, B.E., Bhide, P.G., 2004. Cocaine exposure decreases GABA neuron migration from the ganglionic eminence to the cerebral cortex in embryonic mice. Cereb. Cortex 14, 665–675.
Crawley, J.N., Belknap, J.K., Collins, A., Crabbe, J.C., Frankel, W., Henderson, N., Hitzemann, R.J., Maxson, S.C., Miner, L.L., Silva, A.J., Wehner, J.M., Wynshaw-Boris, A., Paylor, R., 1997. Behavioral phenotypes of inbred mouse strains: implications and recommendations for molecular studies. Psychopharmacology (Berl.) 132, 107–124.
Currie, D.A., de Vente, J., Moody, W.J., 2006. Developmental appearance of cyclic guanosine monophosphate (cGMP) production and nitric oxide responsiveness in embryonic mouse cortex and striatum. Dev. Dyn. 235, 1668–1677.
Curtetti, R., Garbossa, D., Vercelli, A., 2002. Development of dendritic bundles of pyramidal neurons in the rat visual cortex. Mech. Ageing Dev. 123, 473–479.
Cuzon, V.C., Yeh, P.W., Yanagawa, Y., Obata, K., Yeh, H.H., 2008. Ethanol consumption during early pregnancy alters the disposition of tangentially migrating GABAergic interneurons in the fetal cortex. J. Neurosci. 28, 1854–1864.
Daughtrey, W.C., Norton, S., 1982. Morphological damage to the premature fetal rat brain after acute carbon monoxide exposure. Exp. Neurol. 78, 26–37.
Demyanenko, G.P., Halberstadt, A.I., Pryzwansky, K.B., Werner, C., Hofmann, F., Maness, P.F., 2005. Abnormal neocortical development in mice lacking cGMP-dependent protein kinase I. Brain Res. Dev. Brain Res. 160, 1–8.
Di Giovanni, V., Cagiano, R., De Salvia, M.A., Giustino, A., Lacomba, C., Renna, G., Cuomo, V., 1993. Neurobehavioral changes produced in rats by prenatal exposure to carbon monoxide. Brain Res. 616, 126–131.
Ding, J.D., Burette, A., Weinberg, R.J., 2005. Expression of soluble guanylyl cyclase in rat cerebral cortex during postnatal development. J. Comp. Neurol. 485, 255–265.
Duque, A., Rakic, P., 2011. Different effects of bromodeoxyuridine and [3*H*]thymidine incorporation into DNA on cell proliferation, position, and fate. J. Neurosci. 31, 15205–15217.
Erzurumlu, R.S., Gaspar, P., 2012. Development and critical period plasticity of the barrel cortex. Eur. J. Neurosci. 35, 1540–1553.
Fago, A., Mathews, A.J., Dewilde, S., Moens, L., Brittain, T., 2006. The reactions of neuroglobin with CO: evidence for two forms of the ferrous protein. J. Inorg. Biochem. 100, 1339–1343.
Fechter, L.D., Annau, Z., 1977. Toxicity of mild prenatal carbon monoxide exposure. Science 197, 680–682.
Fechter, L.D., Annau, Z., 1980. Prenatal carbon monoxide exposure alters behavioral development. Neurobehav. Toxicol. 2, 7–11.
Furchgott, R.F., Jothianandan, D., 1991. Endothelium-dependent and -independent vasodilation involving cyclic GMP: relaxation induced by nitric oxide, carbon monoxide and light. Blood Vessels 28, 52–61.
Ginsberg, M.D., Myers, R.E., 1976. Fetal brain injury after maternal carbon monoxide intoxication. Clinical and neuropathologic aspects. Neurology 26, 15–23.
Gittins, R., Harrison, P.J., 2004. Neuronal density, size and shape in the human anterior cingulate cortex: a comparison of Nissl and NeuN staining. Brain Res. Bull. 63, 155–160.
Goh, K.L., Cai, L., Cepko, C.L., Gertler, F.B., 2002. Ena/VASP proteins regulate cortical neuronal positioning. Curr. Biol. 12, 565–569.
Gospe Jr., S.M., Zhou, S.S., Pinkerton, K.E., 1996. Effects of environmental tobacco smoke exposure in utero and/or postnatally on brain development. Pediat. Res. 39, 494–498.
Haase, A., Bicker, G., 2003. Nitric oxide and cyclic nucleotides are regulators of neuronal migration in an insect embryo. Development 130, 3977–3987.
Hara, Y., Maeda, Y., Kataoka, S., Ago, Y., Takuma, K., Matsuda, T., 2012. Effect of prenatal valproic acid exposure on cortical morphology in female mice. J. Pharm. Sci. 118, 543–546.

Henninfield, J.E., Goldberg, S.R., 1988. Pharmacologic determinants of tobacco self -administration by humans. Pharmacol. Biochem. Behav. 30, 221–226.
Hu, J.H., Yang, N., Ma, Y.H., Zhou, X.G., Jiang, J., Duan, S.H., Mei, Z.T., Fei, J., Guo, L.H., 2003. Hyperalgesic effects of gamma-aminobutyric acid transporter I in mice. J. Neurosci. Res. 73, 565–572.
Hyde, T.M., Lipska, B.K., Ali, T., Mathew, S.V., Law, A.J., Metitiri, O.E., Straub, R.E., Ye, T., Colantuoni, C., Herman, M.M., Bigelow, L.B., Weinberger, D.R., Kleinman, J.E., 2011. Expression of GABA signaling molecules KCC2. NKCC1, and GAD1 in cortical development and schizophrenia. J. Neurosci. 27, 1234–1311.
Inan, M., Welagen, J., Anderson, S.A., 2012. Spatial and temporal bias in the mitotic origins of somatostatin- and parvalbumin-expressing interneuron subgroups and the chandelier subtype in the medial ganglionic eminence. Cereb. Cortex 22, 820–827.
Jacobowitz, D.M., Heydorn, W.E., 1984. Two-dimensional gel electrophoresis used in neurobiological studies of proteins in discrete areas of the rat brain. Clin. Chem. 30, 1996–2002.
Kallen, K., 2000. Maternal smoking during pregnancy and infant head circumference at birth. Early Hum. Dev. 58, 197–204.
Kawaguchi, Y., Kondo, S., 2002. Parvalbumin, somatostatin and cholecystokinin as chemical markers for specific GABAergic interneuron types in the rat frontal cortex. J. Neurocytol. 31, 277–287.
Kharitonov, S.A., Robbins, R.A., Yates, D.H., Keatings, V., Barnes, P.J., 1995. Acute and chronic effects of cigarette smoking on exhaled nitric oxide. Am. J. Respir. Crit. Care Med. 152, 609–612.
Knipp, S., Bicker, G., 2009. A developmental study of enteric neuron migration in the grasshopper using immunohistochemical probes. Dev. Dynam. 238, 2837–2849.
Krauss, M.J., Morrissey, A.E., Winn, H.N., Amon, E., Leet, T.L., 2003. Microcephaly: an epidemiologic analysis. Am. J. Obstet. Gynecol. 188, 1489–1490, 1484-1489, discussion.
Kriegstein, A.R., 1996. Cortical neurogenesis and its disorders. Curr. Opin. Neurol. 9, 113–117.
Kumada, T., Jiang, Y., Cameron, D.B., Komuro, H., 2007. How does alcohol impair neuronal migration? J. Neurosci. Res. 85, 465–470.
Kumari, V., Soni, W., Mathew, V.M., Sharma, T., 2000. Prepulse inhibition of the startle response in men with schizophrenia: effects of age of onset of illness, symptoms, and medication. Arch. Gen. Psychiatry 57, 609–614.
Laurent, V., Loisel, T.P., Harbeck, B., Wehman, A., Grobe, L., Jackusch, B.M., Wehland, J., Gertler, F.B., Carlier, M.F., 1999. Role of proteins of the Ena/VASP family in actin-based motility of Listeria monocytogenes. J. Cell Biol. 144, 1245–1258.
Lee, C.T., Chen, J., Worden, L.T., Freed, W.J., 2011. Cocaine causes deficits in radial migration and alters the distribution of glutamate and GABA neurons in the developing rat cerebral cortex. Synapse 65, 21–34.
Longo, L.D., 1970. Carbon monoxide in the pregnant mother and fetus and its exchange across the placenta. Ann. N. Y. Acad. Sci. 174, 312–341.
Mactutus, C.F., Fechter, L.D., 1984. Prenatal exposure to carbon monoxide: learning and memory deficits. Science 223, 409–411.
Mactutus, C.F., Fechter, L.D., 1985. Moderate prenatal carbon monoxide exposure produces persistent, and apparently permanent, memory deficits in rats. Teratology 31, 1–12.
McCarthy, D.M., Zhang, X., Darnell, S.B., Sangrey, G.R., Yanagawa, Y., Sadri-Vakili, G., Bhide, P.G., 2011. Cocaine alters BDNF expression and neuronal migration in the embryonic mouse forebrain. J. Neurosci. 31, 13400–13411.
Mereu, G., Cammalleri, M., Fa, M., Francesconi, W., Saba, P., Tattoli, M., Trabace, L., Vaccari, A., Cuomo, V., 2000. Prenatal exposure to a low concentration of carbon monoxide disrupts hippocampal long-term potentiation in rat offspring. J. Pharmacol. Exp. Ther. 294, 728–734.
Milberger, S., Biederman, J., Faraone, S.V., Jones, J., 1998. Further evidence of an association between maternal smoking during pregnancy and attention deficit hyperactivity disorder: findings from a high-risk sample of siblings. J. Clin. Child Psychol. 27, 352–358.
Miller, M.W., Nowakowski, R.S., 1988. Use of bromodeoxyuridine-immunohistochemistry to examine the proliferation, migration and time of origin of cells in the central nervous system. Brain Res. 457, 44–52.
Nakamura, K., Itoh, K., Sugimoto, T., Fushiki, S., 2007. Prenatal exposure to bisphenol A affects adult murine neocortical structure. Neurosci. Lett. 420, 100–105.
Neuner, I., Stocker, T., Kellermann, T., Ermer, V., Wegener, H.P., Eickhoff, S.B., Schneider, F., Shah, N.J., 2010. Electrophysiology meets fMRI: neural correlates of the startle reflex assessed by simultaneous EMG-fMRI data acquisition. Hum. Brain Mapp. 31, 1675–1685.
Noctor, S.C., Scholnicoff, N., Juliano, S.L., 1997. Histogenesis of ferret somatosensory cortex. J. Comp. Neurol. 387, 179–193.
Noctor, S.C., Palmer, S.L., Hasling, T., Juliano, S.L., 1999. Interference with the development of early generated neocortex results in disruption of radial glia and abnormal formation of neocortical layers. Cereb. Cortex 9, 121–136.
Pang, T., Atefy, R., Sheen, V., 2008. Malformations of cortical development. Neurologist 14, 181–191.
Paylor, R., Crawley, J.N., 1997. Inbred strain differences in prepulse inhibition of the mouse startle response. Psychopharmacology (Berl.) 132, 169–180.
Pinho, A.P., Aerts, D., Nunes, M.L., 2008. Risk factors for sudden infant death syndrome in a developing country. Revista de Saude Pub. 42, 396–401.
Poluch, S., Jablonska, B., Juliano, S.L., 2008. Alteration of interneuron migration in a ferret model of cortical dysplasia. Cereb. Cortex 18, 78–92.
Price, D.J., Aslam, S., Tasker, L., Gillies, K., 1997. Fates of the earliest generated cells in the developing murine neocortex. J. Comp. Neurol. 377, 414–422.
Robertson, C.P., Gibbs, S.M., Roelink, H., 2001. cGMP enhances the sonic hedgehog response in neural plate cells. Dev. Biol. 238, 157–167.
Sawai, H., Makino, M., Mizutani, Y., Ohta, T., Sugimoto, H., Uno, T., Kawada, N., Yoshizato, K., Kitagawa, T., Shiro, Y., 2005. Structural characterization of the proximal and distal histidine environment of cytoglobin and neuroglobin. Biochemistry 44, 13257–13265.
Song, H., Ming, G., He, Z., Lehmann, M., McKerracher, L., Tessier-Lavigne, M., Poo, M., 1998. Conversion of neuronal growth cone responses from repulsion to attraction by cyclic nucleotides. Science 281, 1515–1518.
Storm, J.E., Fechter, L.D., 1985. Alteration in the postnatal ontogeny of cerebellar norepinephrine content following chronic prenatal carbon monoxide. J. Neurochem. 45, 965–969.
Storm, J.E., Valdes, J.J., Fechter, L.D., 1986. Postnatal alterations in cerebellar GABA content. GABA uptake and morphology following exposure to carbon monoxide early in development. Dev. Neurosci. 8, 251–261.
Tao, R., Li, C., Newburn, E.N., Ye, T., Lipska, B.K., Herman, M.M., Weinberger, D.R., Kleinman, J.E., Hyde, T.M., 2012. Transcript-specific associations of SLC12A5 (KCC2) in human prefrontal cortex with development. schizophrenia, and affective disorders. J. Neurosci. 32, 5216–5222.
Tegenge, M.A., Bicker, G., 2009. Nitric oxide and cGMP signal transduction positively regulates the motility of human neuronal precursor (NT2) cells. J. Neurochem. 110, 1828–1841.
Toro, R., Leonard, G., Lerner, J.V., Lerner, R.M., Perron, M., Pike, G.B., Richer, L., Veillette, S., Pausova, Z., Paus, T., 2008. Prenatal exposure to maternal cigarette smoking and the adolescent cerebral cortex. Neuropsychopharmacology 33, 1019–1027.
Van Wagenen, S., Rehder, V., 2001. Regulation of neuronal growth cone filopodia by nitric oxide depends on soluble guanylyl cyclase. J. Neurobiol. 46, 206–219.
Verma, A., Hirsch, D.J., Glatt, C.E., Ronnett, G.V., Snyder, S.H., 1993. Carbon monoxide: a putative neural messenger. Science 259, 381–384.
Ward, C., Lewis, S., Coleman, T., 2007. Prevalence of maternal smoking and environmental tobacco smoke exposure during pregnancy and impact on birth weight: retrospective study using Millennium Cohort. BMC Public Health 7, 81.
Weiss, J., Takizawa, B., McGee, A., Stewart, W.B., Zhang, H., Ment, L., Schwartz, M., Strittmatter, S., 2004. Neonatal hypoxia suppresses oligodendrocyte Nogo-A and increases axonal sprouting in a rodent model for human prematurity. Exp. Neurol. 189, 141–149.
Wojtowicz, J.M., Kee, N., 2006. BrdU assay for neurogenesis in rodents. Nat. Protoc. 1, 1399–1405.
Wonders, C.P., Anderson, S.A., 2006. The origin and specification of cortical interneurons. Nat. Rev. Neurosci. 7, 687–696.
Yozu, M., Tabata, H., Nakajima, K., 2004. Birth-date dependent alignment of GABAergic neurons occurs in a different pattern from that of non-GABAergic neurons in the developing mouse visual cortex. Neurosci. Res. 49, 395–403.